Eur. Phys. J. D **16**, 233–236 (2001)

THE EUROPEAN PHYSICAL JOURNAL D

EDP Sciences

Unsupported lead clusters and electron diffraction

M. Hyslop[1,a], A. Wurl[1], S.A. Brown[1], B.D. Hall[2], and R. Monot[3]

[1] Nanostructure Engineering Science and Technology Group (NEST), and Department of Physics and Astronomy, University of Canterbury, Private Bag 4800, Christchurch, New Zealand
[2] Industrial Research Ltd., Gracefield Rd, Lower Hutt, New Zealand
[3] Institute de Physique Expérimentale, EPFL, 1015 Lausanne, Switzerland

Received 30 November 2000

Abstract. A beam of Pb clusters is produced with the inert gas aggregation method and probed by electron diffraction. Analysis of the diffraction patterns indicates that average cluster size can vary between 3 and 7 nm, according to nucleation conditions. The diffraction patterns from beams with larger average cluster size are very similar to patterns calculated from model decahedron clusters, while those for smaller cluster size do not appear to have simple geometrical face-centred cubic, decahedral, or icosahedral structure.

PACS. 36.40.-c Atomic and molecular clusters – 61.46.+w Nanoscale materials: clusters, nanoparticles, nanotubes and nanocrystals – 61.14.-x Electron diffraction and scattering

1 Introduction

The high proportion of surface atoms in atomic clusters can favour atomic arrangements different to that of the bulk material. Hence, determination of small particle structure, and the size range for which non-bulk structures exist, are important fundamental issues. In many structural measurements on atomic clusters interaction with a substrate or matrix is inevitable, and difficult to quantify. The importance of the surface, in contributing to the stability of atomic cluster structures, makes it desirable to reduce such interaction to a minimum. In this work, unsupported Pb clusters are studied in the gas phase using electron diffraction.

Experimental studies of unsupported 8-10 nm Pb clusters have been reported previously [1,2]. These clusters were identified with the bulk face–centred cubic structure (FCC), but thought to also include amorphous regions [1]. Molecular dynamics (MD) simulations [3] on relaxed cuboctahedal (FCC) and icosahedral lead clusters found that cuboctahedra were energetically favoured for all cluster sizes. This is in contrast to many other FCC metals for which transitions from FCC to icosahedral structures have been predicted [4–6] and observed [7–10]. This evidence that the bulk structure prevails at small cluster sizes is intriguing, and suggests that Pb clusters are in some way different to other more extensively studied FCC metals: Cu [10], Ag [11] and Au [12,13].

In a subsequent study, a MD-simulated quench was performed on a large, liquid, 8217-atom lead droplet. The resulting structure was characterised as "icosahedral-like" [14]. It was not energetically favourable, but was thought to occur due to initial formation of (111) planes at the droplet's surface allowing crystallisation to proceed inwards.

[a] e-mail: m.hyslop@phys.canterbury.ac.nz

2 Experimental procedure

The apparatus in this study is essentially the same as used in previous studies of silver and copper clusters [9,10,15]. Clusters are produced by inert gas aggregation in a source chamber with a variable mixture of He and Ar as the inert gas. Lead is evaporated from a crucible, at temperature T_C, into a gentle flow of inert gas at pressure P_G. The Pb vapour condenses into clusters and the resulting mixture of clusters and inert gas is extracted through a series of nozzles to form a molecular beam. On leaving the final nozzle, the beam is probed by an 80 kV electron beam. The random orientation of the clusters produces a Debye-Scherrer (powder) pattern of diffraction rings which is measured by a pair of linear CCD detectors placed along a diameter of the pattern. A deposition rate meter, downstream of the beam crossing, allows measurement of the material flux.

Experimental diffraction patterns accumulate the scattering from individual clusters produced by the source. Hence, patterns corresponding to different cluster sizes and structures will contribute to the measurement, together with an atomic gas background. We analyse this measured data directly. Kinematical diffraction patterns are calculated, using the Debye equation [16], from ideal polyhedral cluster models for a range of sizes and types of structure. These patterns are combined, with variable weightings, to provide a best match to the experimental

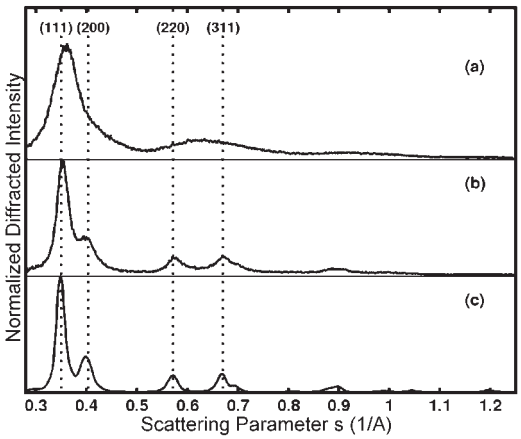

Fig. 1. Diffraction patterns obtained from Pb clusters with different inert gases: (a) pure He and (b) pure Ar. For both patterns $T_C = 810$ °C with $P_G = 5$ mbar and $P_G = 2$ mbar for (a) and (b) respectively. (c) shows the diffraction pattern of a large model decahedron cluster, shown for comparison with experimental patterns from large particles. The positions of the bulk (FCC) peaks for Pb are indicated by the dashed lines.

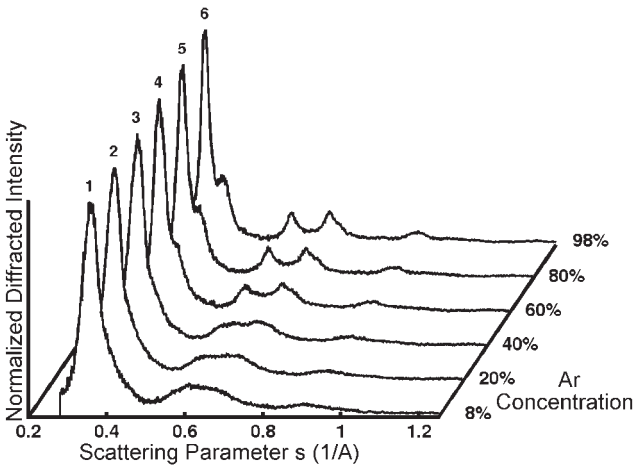

Fig. 2. Diffraction patterns obtained from Pb clusters by increasing the mixing ratio of Ar to He from profile 1 to 6. $T_C = 840$ °C and the total inert gas pressure is ~ 4 mbar.

data. An automatic, robust, fitting procedure is used to obtain this match and estimate uncertainties in the parameters [17]. The procedure is similar, but not identical to, the so-called Debye Functional Analysis (DFA) of X-ray diffraction data [18]. Here, we adopt the term DFA for convenience. The model structures used to calculate basis patterns for the fit are closed-shell geometrical cuboctahedra (FCC), truncated decahedra [4] and icosahedra [4] ranging in size from 55 to 6525 atoms (diameters between roughly 1.5 and 8 nm). Note that both the icosahedron and the decahedron are non-crystalline arrangements of atoms: they are assembled from tetrahedral sub-units and contain twin planes between adjacent tetrahedra, that break the periodicity of the underlying lattice. These two types of structure are collectively referred to as multiply twinned particles (MTP).

In powder diffraction patterns the Scherrer formula [19] is frequently used to estimate particle size. The estimate is calculated from the width of a single diffraction peak, under the assumption that peak broadening is purely due to the limited number of atomic planes in the particle. However, for non-crystalline clusters this generally leads to an incorrect estimate of the cluster size because there is no underlying periodic structure; disorder, and defects also contribute to peak broadening.

A more reliable estimate of the average cluster size can be obtained by Fourier inversion [20] of the diffraction pattern. The diffraction pattern is related to the distribution of inter-atomic distances in a sample by what is essentially a Fourier transform. Thus the diffraction pattern can, in principle, be inverted to regain the inter-atomic distances. Then, from the bound limit to the inter-atomic distances observed, an estimate of sample diameter can be made. Experimentally the diffraction pattern is measured over a limited range of the scattering parameter ($s = 0.3{-}1.2$ Å^{-1}), but Fourier inversion has recently been shown to give a good estimate of the cluster size in spite of this restricted range [20].

Some information about cluster sizes can also be obtained from the results of DFA. DFA assigns a proportion to each of the basis patterns, allowing a volume-weighted average size to be calculated. DFA results, however, are indicative of the size and structure of *domains within* particles and do not necessarily represent the size and structure of *whole* clusters [17]. Therefore, the size information from DFA and from Fourier inversion should be considered complementary, in spite of being derived from the same diffraction data.

3 Results

The range of T_C and P_G for which diffraction patterns can be observed is dependent on the diameter of the nozzle at the exit of the source chamber. This nozzle effectively controls the pressure-flow rate relationship of the inert gas in the source chamber, which in turn affects the cluster production. In this work it is generally the case that diffraction patterns are observed for T_C above ~ 800 °C and for P_G above ~ 0.5 mbar. However, for a given nozzle size and with Ar as the inert gas, clusters are observed at a lower temperature than when He is used. Our results were all obtained using a 6 mm diameter nozzle; a smaller source nozzle increases the T_C required to observe diffraction patterns, but reduces clogging of the second nozzle.

A typical diffraction pattern obtained with pure He as the inert gas is shown in Fig. 1(a). The pattern was obtained for $T_C = 810$ °C and $P_G = 5$ mbar. Even at very high He pressures the asymmetry of the main peak at 0.36 Å^{-1} rarely develops into a prominent shoulder, though the smaller peak centred at 0.62 Å^{-1} is observed to split.

Fig. 1(b) shows a typical diffraction pattern obtained with pure Ar. The pattern was taken for similar conditions

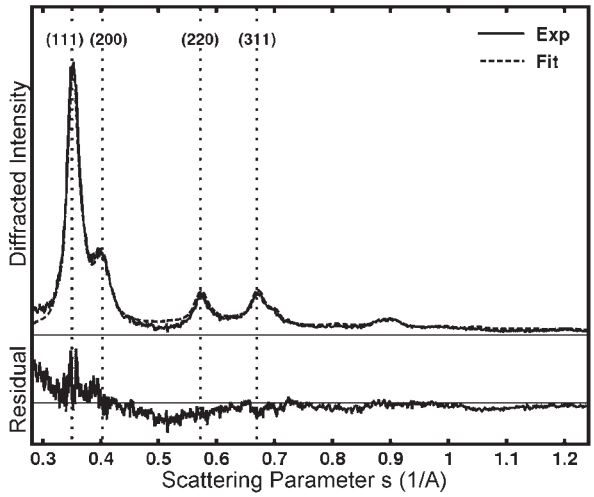

Fig. 3. DFA fit for pattern 6 in Fig. 2. The experimental curve is well matched by the inclusion of large decahedral domains. The lower panel is the difference between experiment and fit (on an expanded scale). The positions of the bulk (FCC) peaks for Pb are indicated by the dashed lines.

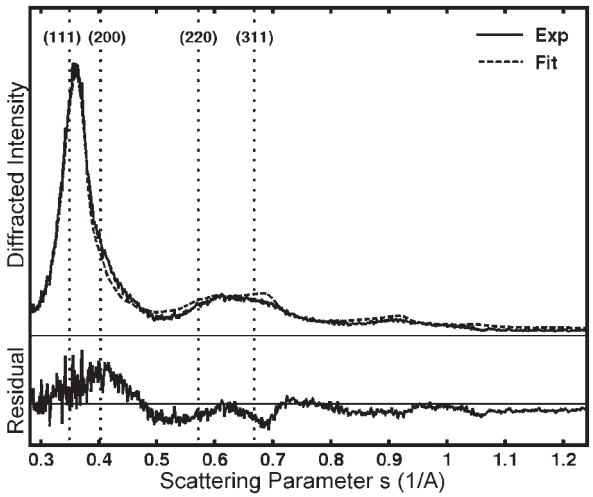

Fig. 4. DFA fit for pattern 1 in Fig. 2. The inability of DFA to accurately reproduce the shapes of the shoulder at 0.4 Å^{-1} and the broad peak centred on 0.62 Å^{-1} indicates that alternative structures must also be considered. The lower panel is the difference between the experiment and fit (on an expanded scale). The positions of the bulk (FCC) peaks for Pb are indicated by the dashed lines.

to Fig. 1(a) with $T_C = 810$ °C and $P_G = 2$ mbar. The main peak at 0.35 Å^{-1} is much sharper than with He and has a well developed shoulder. The peaks at 0.57 Å^{-1} and 0.67 Å^{-1} are always distinct.

Fig. 2 shows a series of diffraction patterns obtained by varying the Ar/He ratio in the source chamber, while keeping the total inert gas pressure at approximately 4 mbar, and with $T_C = 840$ °C. A smooth evolution of diffraction patterns between the two extremes shown in Fig. 1 is observed. The sharpening of features from pattern 1 to pattern 6 suggests an increase in cluster size, and the evolution of the shoulder at ~ 0.4 Å^{-1} indicates a change in the structure of the clusters.

Table 1 summarises the DFA results for patterns 1, 3, 4 and 6 from Fig. 2, as well as size estimations from the 3 available methods. The size estimates from Fourier inversion and DFA are in good agreement, but the Scherrer formula gives lower values, as discussed above.

4 Discussion

Diffraction patterns from Pb clusters have been observed for a range of source conditions, and it is found that the best control over the cluster production is achieved by varying the composition of the inert gas. Results obtained with pure He are significantly different to those obtained with pure Ar, for otherwise identical source conditions. For either gas, only the intensity of the diffraction patterns changes across a wide range of T_C and P_G, which is contrary to behaviour observed with some other metals [2,9,10,15,21,22].

DFA provides a method of characterising the composition of the cluster beam for each of the diffraction patterns observed in Fig. 2. TEM observations [7] often show that individual particles are made up of smaller domains, which may be ordered differently. Diffraction patterns will be dominated by these domains and so DFA results must be considered in this light. Here, the agreement between the size estimates from DFA and Fourier inversion suggests that DFA may be finding the structures that represent most of the clusters' volume. Nevertheless, TEM analysis of the particles is essential before a firm conclusion can be drawn.

The DFA fit for pattern 6 is shown in Fig. 3. The results (Table 1) suggests that pattern 6 is dominated by large decahedron-like domains. The resemblance between diffraction patterns from large decahedral clusters and the experimental pattern is striking (see Fig. 1(c)), but the presence of large decahedra is theoretically unexpected. The experimental diffraction pattern has also been compared (by DFA) to those from other possible structures, such as twinned FCC clusters, however decahedral patterns provide the best fit to the experimental data.

The DFA fit for pattern 1 is shown in Fig. 4. Here, DFA indicates that the domains are predominantly icosahedral. However, DFA does not accurately reproduce the shapes of the shoulder at 0.4 Å^{-1} and the broad peak centred on 0.62 Å^{-1}, which indicates that that the calculated basis patterns could not completely reproduce the cluster structures in the beam: alternative structural models need to be considered as well. A possible refinement would be to use a basis set of relaxed MD-generated structures. Recent MD results, for a variety of metals [12,23,24], suggest that small particles are likely to be imperfect and that amorphous domains may also need to be considered. Unfortunately, alternative structure models for Pb are currently unavailable to us, preventing further investigation at this time.

Table 1. DFA results for experimental patterns 1, 3, 4, and 6 from Fig. 2. The parameter d is the average (volume weighted) domain size for each structure, δ_d is the standard deviation of d, and v is the proportion of each structure (by volume). The size estimates from the 3 available methods are also shown.

		Experimental Profile			
Structure		1	3	4	6
Cuboctahedral	d(nm)	-	-	-	-
	δ_d(nm)	-	-	-	-
	v(%)	0.0	0.0	0.0	0.0
Decahedral	d(nm)	1.9	4.2	7.7	7.5
	δ_d(nm)	0.3	0.6	0.7	1.1
	v(%)	3.5	0.2	14.4	58.5
Icosahedral	d(nm)	2.9	3.4	4.3	3.7
	δ_d(nm)	1.2	1.0	1.4	1.6
	v(%)	96.5	99.8	85.6	41.4
Size estimates	DFA	2.8	3.4	4.8	5.9
(nm)	±0.1				
	Inversion	3.0	3.5	4.0	6.0
	±0.5				
	Scherrer	2.0	2.5	3.0	4.0
	±1.0				

DFA results (Table 1) for patterns 1, 3, 4, and 6 in Fig. 2 show that the composition of the cluster beam changes as the ratio of He and Ar is altered. Compared to pattern 1, there is an increase in average domain size for patterns 3 and 4 (note the appearance of a clear splitting between the peaks at 0.57 $Å^{-1}$ and 0.67 $Å^{-1}$) and the continued dominance of icosahedral domains. DFA of Pattern 4 also reports a population of large decahedral domains. The population of large decahedral domains increases for pattern 6.

Interestingly none of the patterns in Fig. 2 include the bulk FCC structure, contrasting with a previous report [1] which found that slightly larger Pb clusters were exclusively the bulk structure. This may indicate that a transition to bulk structure occurs at a size larger than 7 nm, however structural analysis in the earlier study did not fully consider the possibility of MTP structures.

5 Conclusion

In this study, Pb clusters have been formed by inert gas aggregation using a variable mixture of He and Ar. Clusters with the bulk FCC structure have not been observed in this work. There is a significant difference between the diffraction patterns observed when the inert gas is either pure He or pure Ar. Between these two extremes, a smooth evolution of diffraction features is observed, as He and Ar are mixed. The diffraction patterns obtained with pure Ar strongly resemble the diffraction patterns from model decahedral clusters. Diffraction patterns from small clusters obtained with pure He indicate that cluster structure models other than simple geometric ones must be considered.

Funding for this work was provided by the Marsden Fund, which is administered by the Royal Society of New Zealand.

References

1. A. Yokozeki, J. Chem. Phys. **68**, 3766 (1978).
2. A. Yokozeki, G.D. Stein, J. Appl. Phys. **49**, 2224 (1978).
3. H.S. Lim, C.K. Ong, F. Ercolessi, Surf. Sci. **269/270**, 1109 (1992).
4. S. Ino, J. Phys. Soc. Jap. **27**, 941 (1969).
5. J.E. Hearn, R.L. Johnston, J. Chem. Phys. **107**, 4674 (1997).
6. S. Valkealahti, M. Manninen, Z. Phys. D **26**, 255 (1993).
7. L.D. Marks, Rep. Prog. Phys. **57**, 63 (1994).
8. S. Ino, J. Phys. Soc. Jap. **21**, 346 (1966).
9. D. Reinhard, B.D. Hall, D. Ugarte, R. Monot, Phys. Rev. B **55**, 7868 (1997).
10. D. Reinhard, B.D. Hall, P. Berthoud, S. Valkealahti, R. Monot, Phys. Rev. B **58**, 4917 (1998).
11. S. Giorgio, J. Urban, W. Kunath, Phil. Mag. A **60**, 553 (1989).
12. C.L. Cleveland, U. Landman, T.G. Schaaff, M.N. Shafigullin, P.W. Stephens, R.L. Whetten, Phys. Rev. Lett. **79**, 1873 (1997).
13. K. Heinemann, M.J. Yacaman, C.Y. Yang, H. Poppa, J. Cryst. Growth **47**, 177 (1979).
14. H.S. Lim, C.K. Ong, F. Ercolessi, Comp. Mat. Sci. **2**, 495 (1994).
15. B.D. Hall, M. Flueli, R. Monot, J.-P. Borel, Phys. Rev. B **43**, 3906 (1991).
16. A. Guinier, *X-ray diffraction in crystals, imperfect crystals, and amorphous bodies* (Dover, New York, 1994).
17. B.D. Hall, J. Appl. Phys. **87**, 1666 (2000).
18. W. Vogel, B. Rosner, B. Tesche, J. Phys. Chem. **97**, 11611 (1993).
19. C. Hammond, *The basics of crystallography and diffraction* (Oxford, New York, 1997).
20. B.D. Hall, D. Zanchet, D. Ugarte, J. Appl. Cryst. **33**, 1335 (2000).
21. C.G. Granqvist, R.A. Buhrman, J. Appl. Phys. **47**, 2200 (1976).
22. B.G. de Boer, G.D. Stein, Surf. Sci. **106**, 84 (1981).
23. F. Baletto, C. Mottet, R. Ferrando, Phys. Rev. Lett. **84**, 5544 (2000).
24. K. Michaelian, N. Rendon, I.L. Garzon, Phys. Rev. B **60**, 2000 (1999).